RSC Advances

PAPER

View Article Online
View Journal | View Issue

Cite this: *RSC Adv.*, 2024, **14**, 12278

Synthesis and study of antibiofilm and antivirulence properties of flavonol analogues generated by palladium catalyzed ligand free Suzuki–Miyaura coupling against *Pseudomonas aeruginosa* PAO1†

Anjitha Theres Benny,[a] Masthan Thamim,[a] Prakhar Srivastava,[b] Sindoora Suresh,[a] Krishnan Thirumoorthy,[a] Loganathan Rangasamy,[c] Karthikeyan S.,[d] Nalini Easwaran*[e] and Ethiraj Kannatt Radhakrishnan *[a]

Received 17th December 2023
Accepted 8th April 2024

DOI: 10.1039/d3ra08617h

rsc.li/rsc-advances

The Suzuki–Miyaura coupling is one of the ubiquitous method for the carbon–carbon bond-forming reactions in organic chemistry. Its popularity is due to its ability to undergo extensive coupling reactions to generate a broad range of biaryl motifs in a straightforward manner displaying a high level of functional group tolerance. A convenient and efficient synthetic route to arylate different substituted flavonols through the Suzuki–Miyaura cross-coupling reaction has been explained in this study. The arylated products were acquired by the coupling of a variety of aryl boronic acids with flavonols under $Pd(OAc)_2$ catalyzed reaction conditions in a ligand-free reaction strategy. Subsequently, the antibiofilm and antivirulence properties of the arylated flavonols against *Pseudomonas aeruginosa* PAO1 were studied thoroughly. The best ligands for quorum sensing proteins LasR, RhlR, and PqsR were identified using molecular docking study. These best fitting ligands were then studied for their impact on gene expression level of *P. aeruginosa* by RT-PCR towards quorum sensing genes *lasB*, *rhlA*, and *pqsE*. The downregulation in the gene expression with the effect of synthesized flavonols endorse the antibiofilm efficiency of the compounds.

Introduction

Transition metal-catalyzed reactions are well established as a powerful synthetic tool in the generation of a carbon–carbon or carbon–heteroatom bond.[1–3] This methodology allows the synthetic chemist great access to more functional and complex molecules. The Suzuki–Miyaura cross-coupling acts as one of the best useful methods for the generation of new carbon–carbon (C sp^2–C sp^2) bonds. The best achievement of Suzuki–Miyaura coupling is the stability and low toxicity of organoboron reagents. Additionally, organoboron compounds offer a high selectivity in the cross-coupling reactions substantiating that the Suzuki–Miyaura reaction is good enough for the synthesis of medicinally important new pharmacophores.[4–12]

Flavonols **I** are closed-chain flavonoid subclass most commonly included in our diet. They are generally accepted as exceptional pharmacophores in many biological applications including anticancer,[13] antioxidant,[14] cardioprotective,[15] anti-inflammatory,[16,17] hepatoprotective,[18] antibacterial,[19] and antiviral activities.[20] The additional biological properties exhibited by the flavonols with aryl groups on either A or B ring of the parent flavonol structure generated through Suzuki–Miyaura coupling are the crux of concern in the current study. Among the various biological activities of flavonol the antibiofilm activity is less explored and perhaps best to study due to their significant antibacterial activity. Taking into consideration on the reports of antibiofilm potential of flavonols, a very few flavonols are identified as antibiofilm efficient compounds. Myricetin **II** (ref. 21–25) quercetin **III**,[26,27] morin **IV**,[28] kaempferol **V** (ref. 26 and 27) and isorhamnetin **VII** (ref. 29) are the most studied flavonols with antibiofilm and antivirulence activities (Fig. 1).

[a]*Department of Chemistry, School of Advanced Sciences, Vellore Institute of Technology, Vellore-632014, India. E-mail: ethukr@gmail.com*

[b]*Department of Pharmacy, The Ohio State University, USA*

[c]*Centre for Biomaterials, Cellular and Molecular Theranostics (CBCMT), Vellore Institute of Technology, Vellore-632014, India*

[d]*Department of Biotechnology, School of Bioscience and Technology, Vellore Institute of Technology, Vellore-632014, India*

[e]*Department of Integrative Biology, School of Bioscience and Technology, Vellore Institute of Technology VIT, Vellore-632014, India*

† Electronic supplementary information (ESI) available: Fig. S1–S28. Spectroscopic characterization data of compounds **3(a–g)**. Fig. S29–S84. Spectroscopic characterization data of compounds **5(a–n)**. Fig. S85. Growth curve analysis of *P. aeruginosa* in $\frac{1}{2}$ MIC, $\frac{1}{4}$ MIC, 1/8 MIC dosages of compounds **5(a–n)**. Fig. S86–S90. Molecular docking and molecular dynamic study. CCDC 2054733 and 2122702. For ESI and crystallographic data in CIF or other electronic format see DOI: https://doi.org/10.1039/d3ra08617h

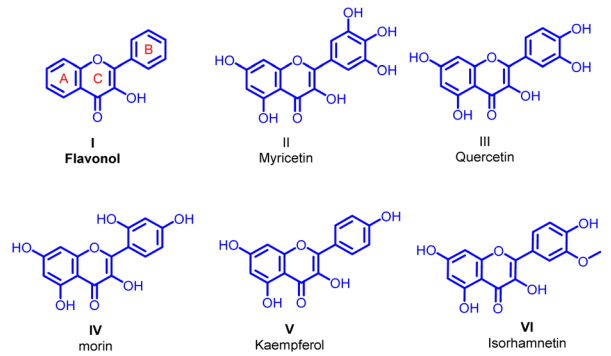

Fig. 1 The general structure of flavonol and reported flavonols with antibiofilm and antivirulence activities.

Biofilm is a stable and complex system with different bacterial colonies or a single type of bacterial group aggregates together in an extracellular polymeric matrix. It can acts as a substantial obstacle to the successful treatment of infectious diseases.[30] They are enclosed in extracellular matrix made up of eDNA, proteins, and polysaccharides that is both protective and impermeable to supplied antibiotics.[31] The physical permeability barrier of the biofilm resists the antibiotics and host immune responses, which makes the antibiotic drugs take a much longer duration to reach their target making the infection more severe.[32] This is the main cause of the development of multidrug-resistant pathogens in the infection site. Biofilm-associated bacteria are particularly difficult to eradicate as they are potent to both host immune responses and common antibiotics. In fact, compared to planktonic bacteria, biofilm removal frequently necessitates treatment with antibiotic doses that are roughly 10–1000 times higher.[33] Quorum sensing (QS) is the process through which bacterial colonies communicate *via* chemical signals, playing a critical role in the development and maturation of biofilms.[34] Therefore, drugs that can disrupt quorum sensing signals hold promise in inhibiting bacterial biofilm development.

Among different biofilm forming bacteria *Pseudomonas aeruginosa* PAO1 is a highly infective pathogenic Gram negative bacteria with high metabolic versatility which will colonize on biotic and abiotic surfaces forming a biofilm.[35] It is an opportunistic bacteria which can cause healthcare infections, such as ventilator-associated pneumonia (VAP), infections in intensive care units, infections at surgical sites, urinary tract infections, burn wound infections, otitis media and keratitis.[36,37] In the case of *P. aeruginosa* the mutants which lack an active QS system are mostly avirulent and incapable of developing into full biofilms.[38] Hence drugs capable of distracting the QS circuits can acts as good biofilm inhibitors. The QS systems of *P. aeruginosa* includes *las*, *rhl* and quinolone-based *pqs* as the most studied systems.[39]

Effective biofilm modulators are still significantly underdeveloped, despite advances in the evaluation of antibacterial efficacy. As a result, we herein describe the generation of a few unreported biaryl flavonols obtained by Suzuki–Miyaura coupling and the evaluation of their anti-biofilm efficiency against *P. aeruginosa* PAO1. We put forward the synthesis, *in vitro* testing, and molecular docking analysis of flavonols against biofilm forming *P. aeruginosa* PAO1. All the synthesized compounds were characterized using various spectroscopic techniques, and utilized for *in vitro* and molecular docking studies. The plausible mechanism of biofilm inhibition was screened by gene expression study of quorum sensing regulated genes *rhlA*, *lasB* and *pqsE* by real time polymerase chain reaction.

Result and discussion

Synthesis of Suzuki-coupled flavonols

5-bromo-2-hydroxyacetophenone **1a**, 2-hydroxyacetophenone **1b**, 5-methyl-2-hydroxyacetophenone **1c** and different substituted benzaldehydes **2(a–g)** were used for the synthesis of flavonols **3(a–g)**. The flavonols were synthesized by the reported Algar–Flynn–Oyamada AFO mechanism with sodium hydroxide as the base and hydrogen peroxide as the oxidizing agent in ethanol–water system[40,41] as depicted in Scheme 1. The reaction proceeded in a one-pot synthetic protocol with chalcone as the intermediate.

The flavonols synthesized were further utilized for the synthesis of biaryl compounds by a ligand-free palladium-catalyzed Suzuki coupling reaction using previous reports.[42] As depicted in Scheme 2 flavonols **3(a–g)** reacts with 1 equiv. of substituted arylboronic acids **4(a–c)** with palladium acetate as catalyst to obtain biaryl flavonols **5(a–n)**. It was further found that the highest yield of 85% was obtained for the generation of biaryl flavonol **5j** (Scheme 3) when the reaction proceeded with K_2CO_3 as the base with 1 : 1 mixture of water DMF as solvent system at 100 °C for 4 h (entry 1, Table 1) and this condition was selected as the optimum condition for the reaction. Other parameters such as reaction time solvent systems with various bases were tried during the optimizations.

Based on the preliminary results, under optimized conditions, the scope of the reaction was explored by synthesising a series of Suzuki coupled products **5(a–n)** from the respective flavonols **3(a–g)** in good yield. All the compounds synthesised were characterized by spectroscopic methods such as FTIR, ^{1}H NMR, ^{13}C NMR, and HRMS, and the spectral data are provided in ESI Fig. S1–84† The compounds **5f** and **5j** were characterized by single crystal XRD and the ORTEP diagram for the compounds are depicted in Fig. 2 and 3. The structures of

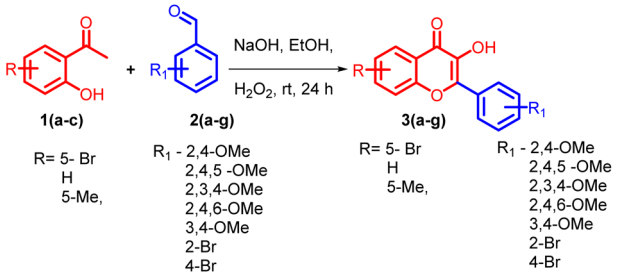

Scheme 1 General scheme for the synthesis of flavonols.

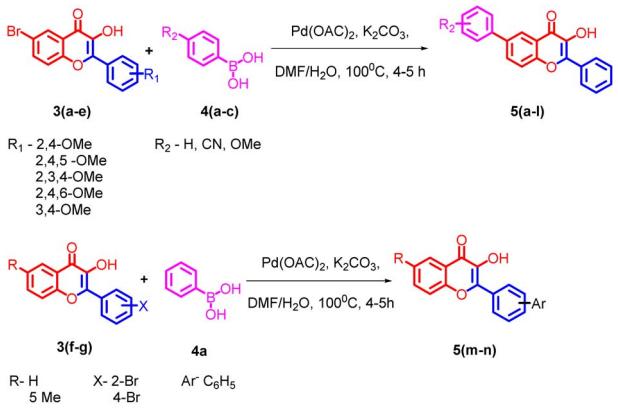

Scheme 2 General scheme for the synthesis of Suzuki-coupled flavonols.

Scheme 3 Optimization for the synthesis **5j**.

Table 1 Optimization for the synthesis **5j**

Entry	Base	Solvent	Temp (°C)	Time (h)	Yield (%)
1	K_2CO_3	DMF/H_2O	100	4	85
2	KOH	DMF/H_2O	100	8	[a]
3	K_2CO_3	DMF	100	5	[a]
4	K_2CO_3	Toluene/*t*-BuOH	80	6	Traces
5	KF	Toluene/*t*-BuOH	80	6	[a]
6	K_2CO_3	THF/H_2O	100	6	Traces
7	Na_2CO_3	Toluene/*t*-BuOH	80	5	Traces

[a] No reaction.

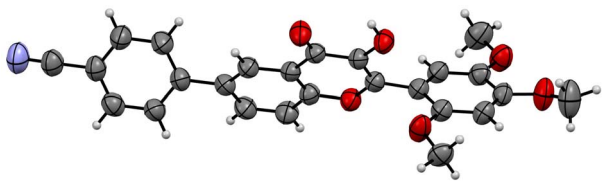

Fig. 2 ORTEP diagram of compound **5f** (CCDC no. 2054733).†

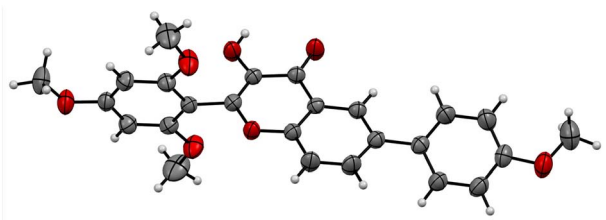

Fig. 3 ORTEP diagram of compound **5j** (CCDC no. 2122702).†

synthesized flavonols **3(a–d)** and Suzuki coupled products **5(a–n)** are represented in Fig. 4.

Determination of minimum inhibitory concentration (MIC)

Table 2 represents the MIC values of all the tested compounds against the bacterial strain. Compounds **5j**, **5l** and **5f**, **5h** show the least minimum inhibitory concentration of 35.9 μM and 36.3 μM against the tested bacterial strain. Gentamicin which was used as the positive control in the experiment shows a minimum inhibitory concentration of 16.3 μM. In detail, the majority of the tested compounds exhibited MIC values below 200 μM. All the further studies including biofilm formation assay and the virulence factor testing were done with the $\frac{1}{4}$ MIC dose of the compounds.

Evaluation of the growth curve

The growth curve of the test microbe at varying concentrations including 1/2 MIC, 1/4 MIC, 1/8 MIC of all the compounds **5(a–n)** was noted in equal intervals for 24 hours. The results for all the compounds are provided in ESI Fig. S85.† The growth curve shows that the compounds did not hamper the normal growth kinetics of the test bacteria with an initial lag phase, subsequent exponential phase and final stationary phase when compared with the untreated control. Hence, the sub-MIC level of the compounds **5(a–n)** was found safe for further assays and we selected $\frac{1}{4}$ MIC dose for all the following experiments.

Prevention of biofilm formation by compounds 5(a–n)

Fig. 5 depicts the impact of sub-MIC levels of compounds **5(a–n)** on inhibiting the formation of biofilm by *P. aeruginosa*, a potent biofilm producer. The results of the biofilm prevention test suggest that the sub-MIC dose of test compounds considerably reduces the ability of tested bacteria to produce biofilms. Greater biofilm formation in drug-untreated wells was noticed with a higher absorbance associated with the drug-untreated microorganisms. However, the relatively lower absorbance in the wells treated with a sub-MIC dose of test compounds

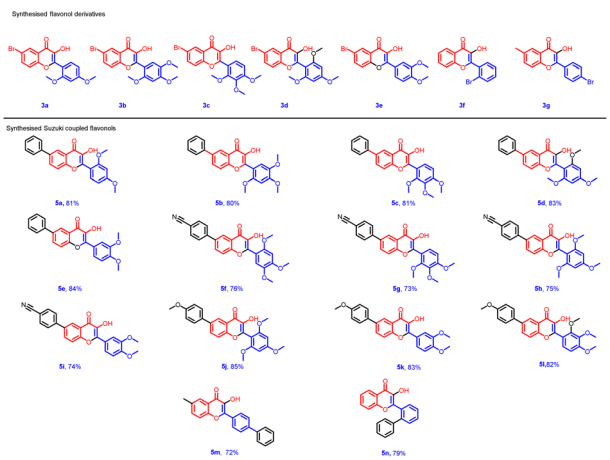

Fig. 4 Structures of synthesized flavonols and Suzuki-coupled flavonols.

Table 2 Minimum inhibitory concentration of compounds 5(a–n)

Flavonols	Minimum inhibitory concentration (μM)
5a	165.6
5b	154.5
5c	154.5
5d	154.5
5e	165.6
5f	36.3
5g	145.5
5h	36.3
5i	156.4
5j	35.9
5k	77.2
5l	35.9
5m	190.3
5n	198.8
Gentamicin	16.3

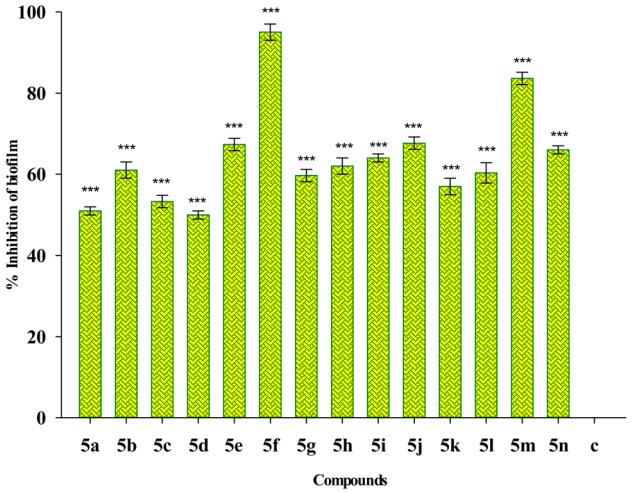

Fig. 5 Effect of treatment of 1/4 MIC dosage of Suzuki coupled flavonol **5(a–n)** on biofilm inhibition of *P. aeruginosa* bacterial biofilm. The results are represented as mean ± SD and analyzed by one-way ANOVA with multiple comparisons *versus* the control group (Dunnett's method). Comparisons were performed among the biofilm production in different Suzuki coupled flavonols and that of the untreated control "(***$p < 0.001$)".

demonstrates a decrease in the production of biofilm. Compound **5f** shows the highest percentage inhibition of 95% among the studied compounds, followed by compound **5m** with a percentage inhibition of 80%. The percentage inhibition of biofilm in other sub MIC concentrations including 1/2 MIC and 1/8 MIC are also included in the ESI Table S1.† The result shows that the higher concentration of the compounds shows a higher percentage reduction in biofilm.

Eradication of preformed biofilm

Biofilm eradication efficiency of Suzuki coupled compounds **5(a–n)** in their sub-MIC doses on preformed biofilm was investigated. All the tested compounds show eradication of the preformed biofilm biomass as represented in Fig. 6. The compound **5g**

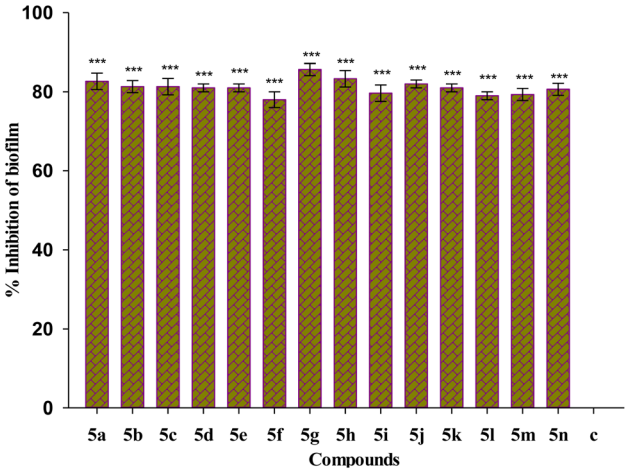

Fig. 6 Effect of treatment of 1/4 MIC dosage of Suzuki coupled flavonol **5(a–n)** on preformed *P. aeruginosa* bacterial biofilm. The results are represented as mean ± SD and analyzed by one-way ANOVA with multiple comparisons *versus* the control group (Dunnett's method). Comparisons were performed among the biofilm production in different Suzuki-coupled flavonols and that of the untreated control (***$p < 0.001$).

shows the maximum percentage inhibition of 86%. All the tested compounds show biofilm eradication above 76%.

Analysis of biofilm architecture

Scanning electron microscopic imaging of *P. aeruginosa* biofilm. The qualitative evaluation of the biofilm morphology was analysed by SEM imaging technique. The method was used to have a comparative analysis of the biofilm architecture of untreated bacterial biofilm and that of flavonol-treated biofilm. *P. aeruginosa* biofilm allowed to grow in sub-MIC dosage of **5f** in culture media showed good inhibition in the biofilm formation and was evident in the electron microscopic image. Compound **5f** was selected among the set of 14 test compounds based on its high biofilm inhibition property compared with other test compounds used in the study. The cell density and morphology of the drug-treated bacterial biofilm were compared with the positive control. The cell density of the compound-treated biofilm was seen highly reduced when compared with the untreated one. Similarly, the cell density was comparable with that of previously reported gentamicin which is a good antibiofilm and antibiotic against Gram-negative *P. aeruginosa* bacteria. Fig. 7 represents the SEM images of the coverslips loaded in biofilm untreated with any drugs, treated with gentamicin (positive control), and biofilm treated with compound **5f**.

Confocal laser scanning microscopic imaging of *P. aeruginosa* biofilm. The CLSM micrographs gave a clear visual evidence on the inhibition of biofilm of *P. aeruginosa* upon treatment with the test compound. A remarkable difference in the morphology and cell density in the biofilm of test bacteria was observed in CLSM with a reduced biofilm formation and scattered bacterial cells. The biofilm architecture without treatment of compound and after treatment of $\frac{1}{4}$ MIC dose of compound **d** are represented in Fig. 8.

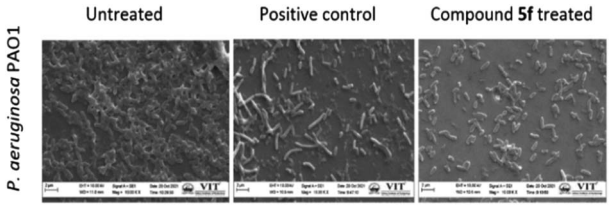

Fig. 7 SEM images of coverslips grown in *P. aeruginosa* biofilm. All the images are at 10.00 k× magnification.

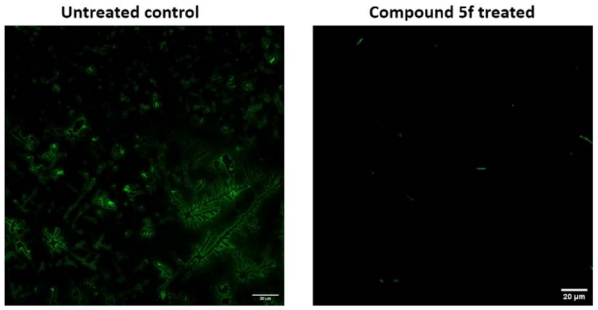

Fig. 8 CLSM images of 72 h grown *P. aeruginosa* biofilm formed on cover slips in the absence of any drugs (control) and in the presence of 1/4 MIC dosage of compound **5f**.

Screening of antibiofilm activity of the compounds

Effect of compounds on pyocyanin production. Pyocyanin is a blue colored redox-active secondary metabolite and virulence factor produced by *P. aeruginosa*. It is found that the concentration of pyocyanin in the sputum of patients with cystic fibrosis infected by *P. aeruginosa* is very high. This implies the correlation of pyocyanin concentration and severity of infection.[43] It can also cause oxidative damage to components of cell cycle as well as direct damage to DNA, NAD(P)H depletion and enzyme inhibition with the main target, the mitochondria of cells.[44] Hence we studied the effect of the compounds on the pyocyanin production in *P. aeruginosa*. It was found that the pyocyanin concentration in the test bacterial culture in untreated control was very high in comparison with the flavonol **5(a–n)** treated culture Fig. 9. All the compounds show a percentage reduction in pyocyanin above 56% and the compound **5n** shows the maximum percentage reduction of 90%. The results suggest that the compounds are capable of inhibiting the production of pyocyanin to a good extend.

Effect of compounds on LasA protease production. LasA protease estimation was done by determining the staphylolytic activity. LasA is involved in host ectodomain shedding which can cause cell surface protein cleavage, leading to disruption of epithelial tissues, tissue penetration and endothelial damage.[45] In the present study we evaluated the effect of flavonols on the production of LasA protease and found that the compounds **5n** and **5m** exhibited maximum percentage inhibition in LasA production. All the test compounds show a good reduction in LasA production ranging from 69% to 72% at it $\frac{1}{4}$ MIC dosages as represented in Fig. 10.

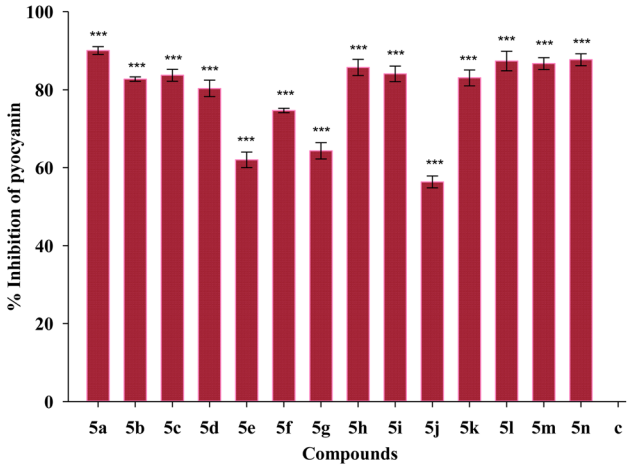

Fig. 9 Effect of treatment of 1/4 MIC dosage of Suzuki coupled flavonol **5(a–n)** on pyocyanin production by *P. aeruginosa* bacterial biofilm. The results are represented as mean ± SD and analyzed by one-way ANOVA with multiple comparisons *versus* the control group (Dunnett's method). Comparisons were performed among the biofilm production in different Suzuki-coupled flavonols and that of the untreated control (***$p < 0.001$).

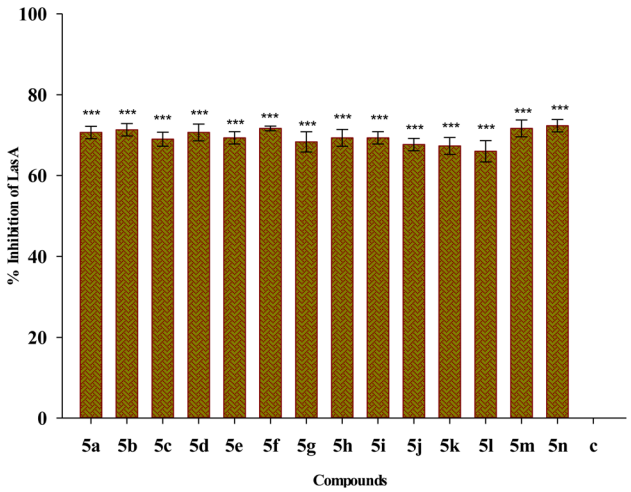

Fig. 10 Effect of treatment of 1/4 MIC dosage of Suzuki coupled flavonol **5(a–n)** on LasA protease production by *P. aeruginosa* bacterial biofilm. The results are represented as mean ± SD and analyzed by one-way ANOVA with multiple comparisons *versus* the control group (Dunnett's method). Comparisons were performed among the biofilm production in different Suzuki-coupled flavonols and that of the untreated control (***$p < 0.001$).

Effect of compounds on cell surface hydrophobicity. The effect of 1/4 MIC levels of compounds **5(a–n)** on cell surface hydrophobicity on *P. aeruginosa* is represented in Fig. 11. Results of the cell surface hydrophobicity showed that sub-MIC dose (1/4 MIC) of the test compounds reduced the cell surface hydrophobicity drastically. Interestingly, among the tested compounds, **5n** displayed a maximum percentage reduction of cell surface hydrophobicity of 85%. The compound **5h** displayed the least percentage reduction among the tested

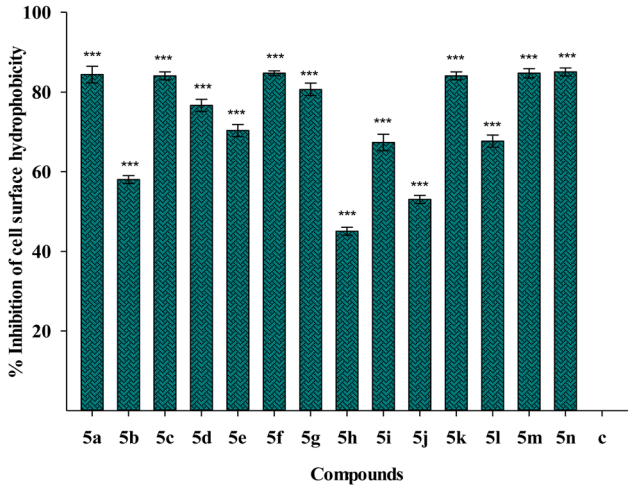

Fig. 11 Effect of treatment of 1/4 MIC dosage of Suzuki coupled flavonol **5(a–n)** on cell surface hydrophobicity of *P. aeruginosa* bacterial biofilm. The results are represented as mean ± SD and analyzed by one-way ANOVA with multiple comparisons *versus* the control group (Dunnett's method). Comparisons were performed among the biofilm production in different Suzuki-coupled flavonols and that of the untreated control (***$p < 0.001$).

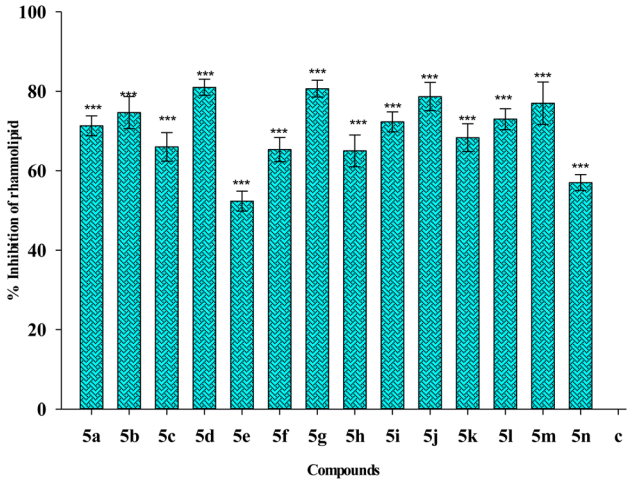

Fig. 12 Effect of treatment of 1/4 MIC dosage of Suzuki coupled flavonol **5(a–n)** on rhamnolipid production by *P. aeruginosa* bacterial biofilm. The results are represented as mean ± SD and analyzed by one-way ANOVA with multiple comparisons *versus* the control group (Dunnett's method). Comparisons were performed among the biofilm production in different Suzuki-coupled flavonols and that of the untreated control (***$p < 0.001$).

compounds and it shows a percentage inhibition of 54%. As the compounds can reduce the hydrophobicity of the bacteria it can thereby inhibit the initial attachment of the bacteria on hydrophobic surfaces including medical implants and hence the further development to a matured biofilm.

Effect of compounds on rhamnolipid production. Rhamnolipid is a bio surfactant produced by *P. aeruginosa*. It acts as a wetting agent and it is essential for bacterial surface dissemination called swarming motility and for normal biofilm development.[30] We studied the effect of flavonols **5(a–n)** on the production of this virulence factor and found that the compounds are capable of inhibiting the rhamnolipid production. Among the tested compounds, compound **5d** shows a maximum reduction level of 81% in rhamnolipid production. The effect of $\frac{1}{4}$ MIC of flavonol **5(a–n)** in the reduction of rhamnolipid production of *P. aeruginosa* tested by orcinol method is graphically plotted in Fig. 12.

Effect of compounds on gene expression of *P. aeruginosa* real time-polymerase chain reaction. Gene expression analyses of *rhlA*, *lasB*, and *pqsE* genes were studied to find the effect of treatment of Suzuki-coupled flavonols with biofilm-forming *P. aeruginosa* biofilm. Among the set of fourteen compounds **5f** and **5m** were selected for the RT-PCR study. **5f** and **5m** were found as best among other test compounds in static biofilm inhibition assay and eradication of preformed biofilm assay. Similarly, these compounds were found to have good antivirulence activity in all the virulence assays carried out in the study. The gene expression study shows that the treatment of *P. aeruginosa* biofilm with the test compounds significantly downregulates the expression of *rhlA*, *lasB*, and *pqsE* genes as represented in Fig. 13A–C. The downregulation of these genes implies the inhibition of biofilm formation by the inhibition of quorum sensing and biofilm formation.

Cytotoxicity of the compounds – MTT assay. The cytotoxicity of the compounds were evaluated by MTT assay using one of the model compound **5f** which was showing the highest efficiency in antibiofilm assay. The results suggest that the compound is safe to use in normal cells up to 100 μM concentration. The concentration of compound used in antibiofilm, antivirulence and gene expression studies were 1/4 MIC value which was very less than 100 μM. The results were compared with standard drug cisplatin and found that the IC_{50} value of the compound at 24 h and 48 h was >100 μM and that of the standard drug cisplatin as >50 μM, the IC_{50} values of the compound and that of cisplatin is included in Table 3.

Molecular docking. The mode of binding in the designated binding site of quorum-sensing receptors was predicted by molecular docking. Molecular docking studies were performed on the ligands **5f** and **5m** which were showing high percentage reduction in biofilm in *in vitro* study. It was found that the chosen receptors were unable to produce any binding modes in response to ligand **5f** even though the compound was showing high antibiofilm activity in *in vitro* study. A highest score was shown by compound **5m** with a binding affinity of -9.247 kcal mol^{-1} against 2UV0 and -8.415 kcal mol^{-1} against 8QD0. The docking scores of the ligands **5m** and **5f** with the respective proteins are represented in Table 4. In order to comprehend the geometry of binding and the interactions that resulted, the poses of the molecule were next examined. The **2d** and **3d** interactions of the ligand **5m** with the proteins 2UV0 and 8QD0 are represented in Fig. 14a–d as they are having highest docking score.

Molecular dynamics. The molecular dynamic study was performed for the ligand **5m** with the respective quorum sensing receptor proteins. The dynamics of 2UV0-**5m**, 4JVI-**5m**, and 8DQ0-**5m** complexes were studied to understand the

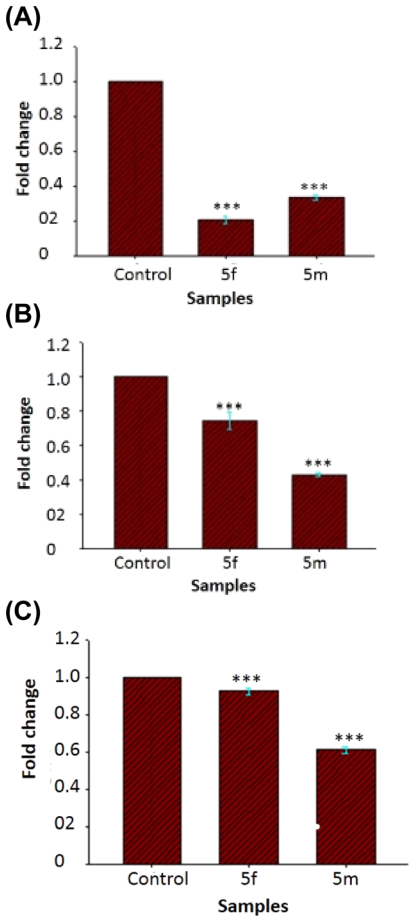

Fig. 13 (A) Gene expression levels of *P. aeruginosa* biofilm treated with compounds **5f** and **5m** against *lasB*. The results are represented as mean ± SD and analyzed by one-way ANOVA with multiple comparisons *versus* the control group (Dunnett's method). Comparisons were performed within the gene expression level of different esters and that of the untreated control "(***$p < 0.001$)". (B) Gene expression levels of *P. aeruginosa* biofilm treated with compounds **5f** and **5m** against *rhlA*. The results are represented as mean ± SD and analyzed by one-way ANOVA with multiple comparisons *versus* the control group (Dunnett's method). Comparisons were performed within the gene expression level of different esters and that of the untreated control "(***$p <$ 0.001)". (C) Gene expression levels of *P. aeruginosa* biofilm treated with compounds **5f** and **5m** against *pqsE*. The results are represented as mean ± SD and analyzed by one-way ANOVA with multiple comparisons *versus* the control group (Dunnett's method). Comparisons were performed within the gene expression level of different esters and that of the untreated control "(***$p < 0.001$)".

Table 3 *In vitro* cytotoxicity assay conducted for compound **d** on HEK 293 cells

Compound	IC_{50} at 24 h (μM)	IC_{50} at 48 h (μM)
5f	>100 μM	>100 μM
Cisplatin	>50 μM	>50 μM

conformation stability during the binding process. The structural alterations were assessed using two parameters, including RMSD and RMSF. The stability of each complex was calculated

Table 4 Docking score of lead molecules interacting with quorum-sensing receptors (PDB IDs 2UV0, 4JVI, 8DQ0)

Protein	Ligand	Docking score
2UV0	**5m**	−9.247
2UV0	**5f**	NP
4JVI	**5m**	−5.457
4JVI	**5f**	NP[a]
8QD0	**5m**	−8.415
8QD0	**5f**	−5.988

[a] NP – no pose generated.

using RMSD of the Cα atoms of the protein structure. It was found that the 2UV0-**5m** complex has the minimum structural deviation with an RMSD value of 1.75 Å and ligand had 0.75 Å Fig. 15a, whereas the 4UJI-**5m** and 8DQ0-**5m** complexes had higher RMSD values as depicted in ESI Fig. S86(a and b).† This suggests that, compared to other complexes, the 2UV0-**5m** complex has the least amount of conformational changes induced by ligands.

To further understand the conformational change, we studied the RMSF to evaluate the protein residue fluctuation and the RMSF plot of 2UV0 protein with binding site is depicted in Fig. 15b.The RMSF plots of other proteins are included in ESI Fig. S86(c and d).† It was noted that structural alterations to the binding site had an impact on the RMSD of the 4JVI-**5m** and 8DQ0-**5m** complexes. Since the important factor for producing activity and structural stability is the interaction between protein and ligand, we have assessed the bonded interaction of the complexes. The protein ligand interaction of the complex 8DQ0-**5m** is represented in the histogram Fig. 15c and the protein ligand interactions of other complexes are included in ESI Fig. S87(a and b).† Among all the three complexes, 8DQ0-**5m** was more stable. It has hydrophobic interaction with TYR64 and TRP96, hydrogen bonding with ALA83, and water-mediated hydrogen bonding with ASP81, and THR121. We observed that the 2UV0-**5m** and 4JVI-**5m** complexes were having TRP60 and ARG209 respectively as maintained interaction throughout the 200 ns simulation.

Binding free energy calculation. Molecular Mechanics based Generalized Born and Surface Area (MM-GBSA) method was used to find the binding free energy of complex in each snapshot extracted from MD trajectory in 20 ns intervals. The MM-GBSA energy was used to estimate the binding affinity of the ligand towards the protein. During the simulation phase, the influence of conformational changes in binding free energy was evaluated. It was observed that the 8DQ0-**5m** complex has attained maximum energy due to its feasible geometrical orientation leading to the most stable conformer in the simulation event while the other complexes have lesser energy. Further going forward to 200 ns the binding free energy was not showing any huge deviations. Interactions of ligands with the proteins in 20 ns interval frames of 200 ns simulation study are incorporated in ESI Fig. S88–S90.† The binding free energy distribution for the selected frames of **5m** and 8DQ0 is included

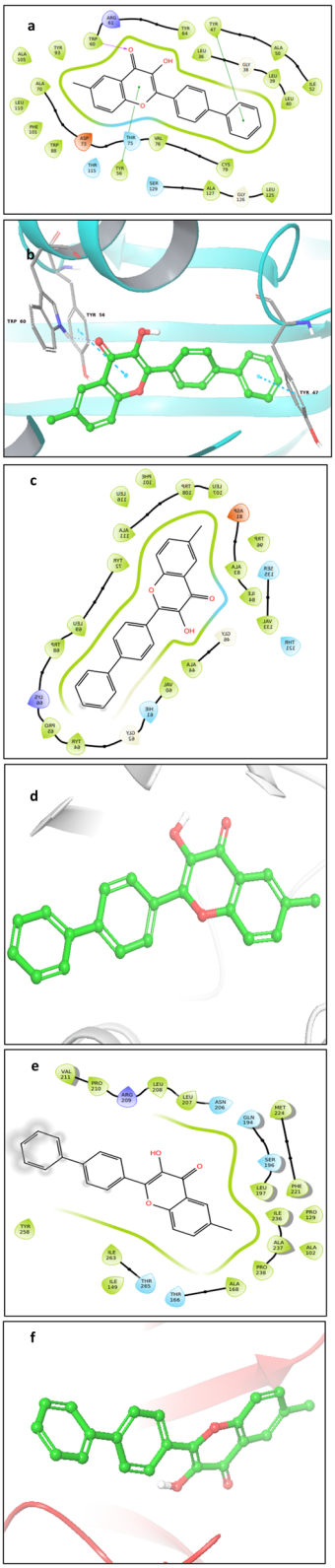

Fig. 14 (a–d) Interactions of **5m** ligand with quorum-sensing receptors (a) 2D interaction of 2UV0 with **5m** ligand (b) 3D interaction of 2UV0 with **5m** ligand (c) 2D interaction of 8DQ0 with **5m** ligand (d) 3D interaction of 8DQ0 with **5m** ligand (e) 2D interaction of 4JVI with **5m** ligand (f) 3D interaction of 4JVI with **5m** ligand.

in Table 5 and for the complexes **5m**-2UV0 and **5m**-4JVI are included in the ESI Tables S2 and S3.†

The molecular docking analysis failed to demonstrate any pose between **5f** and the receptor proteins 2UV0 and 4JVI in the *in silico* tests, which is in contrast to the *in vitro* results where **5f** shown the best antibiofilm action. The compound **5m** which shows 80% inhibition in the biofilm formation was showing interesting results in the molecular docking and molecular dynamic studies. Even though the molecular docking results give a more negative binding affinity for the interaction of **5m** with 2UV0, the molecular dynamic study shows the **5m**-8DQ0 complex as more stable. It can possibly due to the more stable and strong interactions between the ligand and protein. Similarly the effect of compound **5m** on gene expression of the *P. aeruginosa* also supports the molecular dynamic results with a very high downregulation of *rhlA* gene.

Materials and methods

General

All the reactions were carried out in oven-dried glasswares. 2-Hydroxyacetophenones, substituted benzaldehydes, palladium acetate, and substituted boronic acids were purchased from Sigma Aldrich and used as received. Progress of reactions was monitored by the silica gel Thin Layer Chromatography (TLC) technique. Purification of crude compounds was done by column chromatography using silica gel (mesh size 100–200). The NMR spectra were recorded on Bruker-400 MHz NMR spectrometer (400 MHz for ^{1}H NMR and 100 MHz for ^{13}C NMR) with $CDCl_3$ as the solvent and TMS as an internal reference. Integrals are in accordance with assignments; coupling constants (J) were reported in Hertz (Hz). All ^{13}C spectra are proton-decoupled. Multiplicity is indicated as follows: s (singlet), d (doublet), t (triplet), q (quartet), m (multiplet), dd (doublet of doublet), br s (broad singlet). HRMS analyses were recorded using high-resolution mass spectrometer. Yields refer to quantities obtained after chromatography. All the commercial solvents were purified before use.

Bacterial strains and chemicals. *Pseudomonas aeruginosa* PAO1 and *Staphylococcus aureus subsp. aureus*, MTCC no: 1430 strains were obtained from MTCC, CSIR-Institute of Microbial Technology, Chandigarh, India, and cultured when necessary. Fresh subcultures were prepared each time. TRIzol, TB green premix Ex Taq II (Tli RNase H) plus, and prime script RT reagent kit (Perfect Real Time) to generate cDNA for real-time PCR were purchased from Takara. Primers used were purchased from Eurofins Genomics India Pvt., Ltd. All the other chemicals, solvents, and reagents used for the quantification of virulence factors were procured from Sigma Aldrich chemicals.

General procedure for the synthesis of flavonols 3(a–g). Flavonols were synthesized by the synthetic procedure used in our previous publication.[46] A 50 mL RB flask was charged with substituted 2-hydroxyacetophenones **1(a–c)** (1 mmol) and a solution of NaOH (0.64 g) in ethanol (9.6 mL) at room temperature was added to this and kept for stirring for 5

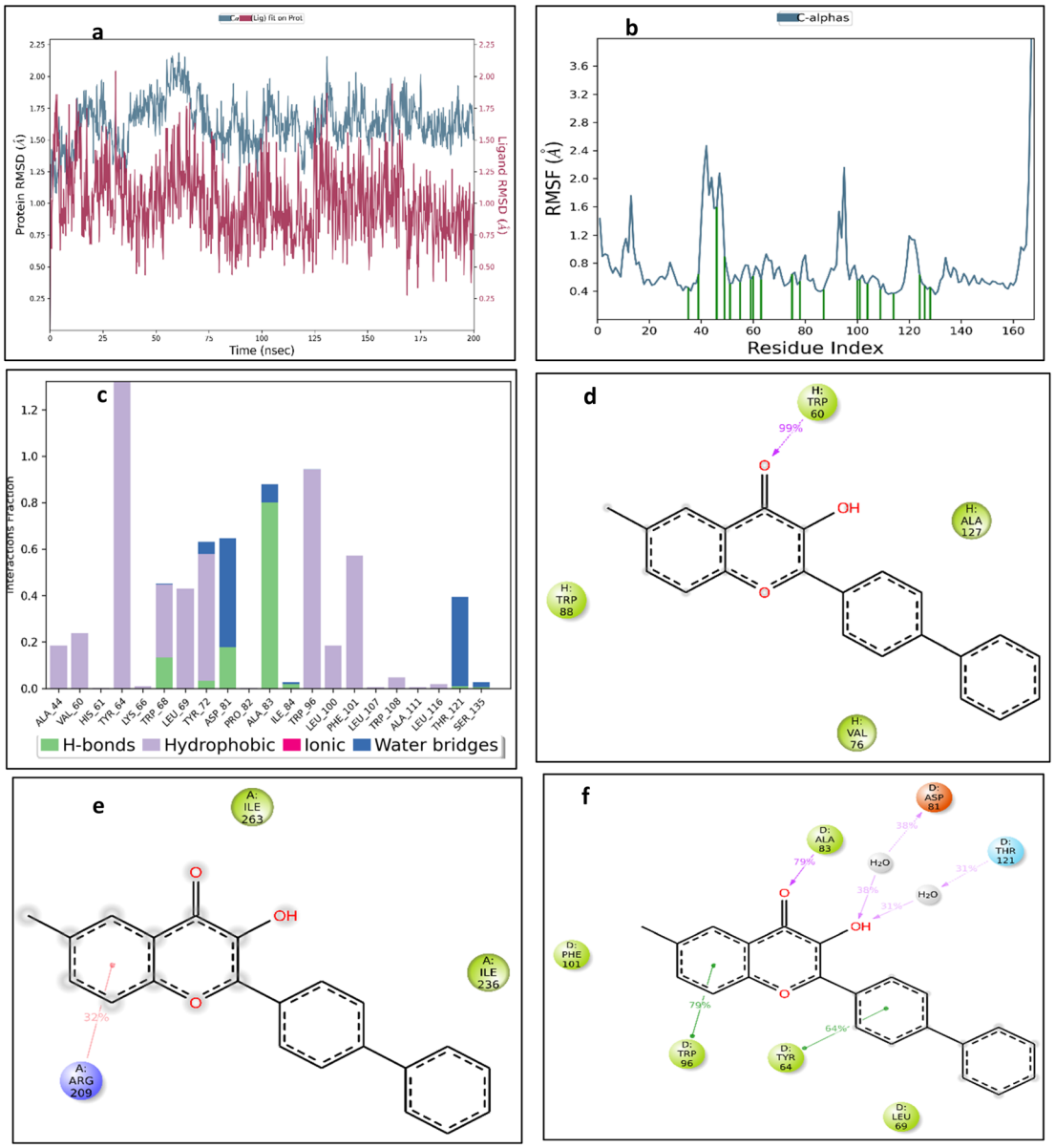

Fig. 15 (a) 2UV0-**5m** complex RMSD (b) RMSF of 2UV0 protein with binding site marked in green lines (c) 8DQ0-**5m** complex interaction histogram (d) 2UV0-**5m** complex interactions maintained (e) 4JVI-**5m** complex interactions maintained (f) 8DQ0-**5m** complex interactions maintained.

minutes. Substituted benzaldehydes **2(a–f)** (1.05 mmol) were then added and the mixture was continued stirring for 24 hours. After 24 hours, 10 mL of distilled water and 0.27 mL of 30% hydrogen peroxide were added to it. This mixture was continued stirring for another 24 hours. The progress of the reaction was monitored by TLC using 15% ethyl acetate–hexane. The reaction was quenched with ice. The resulting yellow solid was filtered washed with water, and dried to yield the final product. The crude product was purified by silica gel column chromatography to afford pure products **3(a–g)**. Eluent (hexane/ethyl acetate 10–20%). The products **3(a–g)** obtained were characterized by spectroscopic techniques.

*6-Bromo-2-(2,4-dimethoxyphenyl)-3-hydroxy-4H-chromen-4-one (**3a**).* Yellow solid; yield: 90%; FTIR (KBr) ν_{max}: 3446, 1573, 1496, 1278, 1107, 927, 790 cm^{-1}; ^1H NMR (400 MHz, $CDCl_3$/TMS): δ 8.39 (d, $J = 2.4$ Hz, 1H), 7.73 (dd, $J = 11.2$ Hz, 1H), 7.52 (d, $J = 8.4$ Hz, 1H), 7.40 (d, $J = 8.8$ Hz, 1H), 6.64 (dd, $J = 10.4$ Hz, 1H), 6.59 (d, $J = 2$ Hz, 1H), 6.35 (s, 1H), 3.87 (s, 3H), 3.85 (s, 3H); ^{13}C NMR (100 MHz, $CDCl_3$/TMS): 172.1, 163.2, 158.9, 154.7, 146.8, 138.9, 136.2, 132.5, 128.0, 122.8, 120.5, 117.7, 112.1, 105.2, 99.3, 56.0, 55.7; HRMS: $C_{17}H_{13}BrO_5$ m/z $[M + H]^+$: calculated: 377.0024, found: 377.0046.

*6-Bromo-3-hydroxy-2-(2,4,5-trimethoxyphenyl)-4H-chromen-4-one (**3b**).* Yellow solid; yield: 85%; FTIR (KBr) ν_{max}: 3294, 2937, 1600, 1570, 1209, 1161, 1107, 813, 721, 680 cm^{-1}; ^1H NMR (400 MHz, $CDCl_3$/TMS): 8.39 (s, 1H), 7.72 (d, $J = 8.8$ Hz, 1H), 7.40 (d, $J = 7.6$ Hz, 1H), 7.10 (s, 1H), 6.64 (s, 1H), 6.52 (s, 1H), 6.45 (s, 1H), 3.96 (s, 3H), 3.87 (s, 6H); ^{13}C NMR (100 MHz, $CDCl_3$/TMS):

Table 5 8DQ0-**5m** complex binding free energy distribution for the selected frames

	Frame	Δ*G* coulomb	Δ*G* covalent	Δ*G* H-bond	Δ*G* lipo	Δ*G* packing	Δ*G* Solv_GB	Δ*G* vdW	Δ*G* bind
8DQ0-**5m**	0 ns	−5.82	4.62	−1.50	−36.51	−9.29	17.35	−50.74	−81.91
8DQ0-**5m**	20 ns	−20.18	6.94	−2.44	−37.28	−9.00	20.26	−54.18	−95.90
8DQ0-**5m**	40 ns	−13.73	5.91	−2.46	−34.62	−10.98	20.15	−61.61	−97.35
8DQ0-**5m**	60 ns	−14.06	6.62	−2.21	−34.73	−9.84	13.15	−59.03	−100.12
8DQ0-**5m**	80 ns	−35.39	6.65	−1.55	−37.34	−11.80	24.78	−53.93	−108.60
8DQ0-**5m**	100 ns	−24.54	3.55	−2.80	−31.80	−13.25	22.19	−51.80	−98.47
8DQ0-**5m**	120 ns	−27.80	3.19	−1.71	−34.25	−14.46	24.59	−54.84	−105.29
8DQ0-**5m**	140 ns	−39.59	10.64	−1.54	−35.76	−13.19	30.67	−55.81	−104.58
8DQ0-**5m**	160 ns	−18.34	5.34	−1.17	−37.23	−15.03	21.31	−58.42	−103.56
8DQ0-**5m**	180 ns	−14.41	5.99	−1.43	−36.45	−13.58	15.51	−62.39	−106.77
8DQ0-**5m**	200 ns	−27.49	6.07	−1.08	−36.76	−11.65	26.45	−58.32	−102.79

170.9, 153.5, 151.5, 151.1, 145.3, 142.2, 137.7, 135.1, 126.9, 121.7, 119.3, 116.5, 112.2, 109.5, 96.9, 55.9, 55.5, 55.1; HRMS: $C_{18}H_{15}BrO_6$ *m*/*z* $[M + H]^+$: calculated: 407.013, found: 407.0128.

*6-Bromo-3-hydroxy-2-(2,3,4-trimethoxyphenyl)-4H-chromen-4-one (**3c**).* Yellow solid; yield: 88%; FTIR (KBr) ν_{max}: 3363, 2937, 1591, 1440, 1400, 1282, 1097, 864, 794 cm^{-1}; ^1H NMR (400 MHz, $CDCl_3$/TMS): δ 8.40 (s, 1H), 7.75 (d, $J = 8.6$ Hz, 1H), 7.41 (d, $J = 9.2$ Hz, 1H), 7.35 (d, $J = 8.8$ Hz, 1H), 6.82 (d, $J = 8.4$ Hz, 1H), 6.68 (d, $J = 8.4$ Hz, 1H), 3.96 (s, 3H), 3.93 (s, 3H), 3.91 (s, 1H); ^{13}C NMR (100 MHz, $CDCl_3$/TMS): 152.3, 146.2, 136.2, 128.0, 125.6, 122.7, 120.2, 107.3, 61.6, 60.9, 56.1, 29.7; HRMS: $C_{18}H_{15}BrO_6$ *m*/*z* $[M + H]^+$: calculated: 407.0130, found: 407.0130.

*6-Bromo-3-hydroxy-2-(2,4,6-trimethoxyphenyl)-4H-chromen-4-one (**3d**).* Yellow solid; yield: 89%; FTIR (KBr) ν_{max}: 3269, 2933, 1598, 1583, 1452, 1203, 1114, 815, 661 cm^{-1}; ^1H NMR (400 MHz, $CDCl_3$/TMS): δ 8.40 (s, 1H), 7.724 (d, $J_{12} = 2.4$ Hz, $J_{14} = 9.2$ Hz, 1H), 7.40 (d, $J = 9.2$ Hz, 1H), 6.22 (s, 2H), 6.15 (s, 1H), 3.95 (s, 3H), 3.87 (s, 3H), 3.78 (s, 3H); ^{13}C NMR (100 MHz, $CDCl_3$/TMS): 172.0, 163.8, 159.6, 155.1, 144.3, 140.2, 135.9, 127.8, 122.9, 120.6, 117.3, 90.8, 56.0, 55.5; HRMS: $C_{18}H_{15}BrO_6$ *m*/*z* $[M + H]^+$: calculated: 407.0130, found: 407.0136.

*6-Bromo-2-(3,4-dimethoxyphenyl)-3-hydroxy-4H-chromen-4-one (**3e**).* Yellow solid; yield 86%; FTIR (KBr) ν_{max}: 3271, 1587, 1471, 1220, 864, 736, 680 cm^{-1}; ^1H NMR (400 MHz, $CDCl_3$/TMS): δ 8.39 (d, $J = 2.4$ Hz, 1H), 7.74 (dd, $J = 2.4$ Hz, 8.8 Hz, 1H), 7.53 (d, $J = 8.4$ Hz, 1H), 7.41 (d, $J = 9.2$ Hz, 1H), 6.65 (dd, $J = 2$ Hz, 8.4 Hz, 1H), 6.59 (d, $J = 2.0$ Hz, 1H), 6.39 (s, 1H), 3.88 (s, 3H), 3.85 (s, 3H); ^{13}C NMR (100 MHz, $CDCl_3$/TMS): 172.1, 163.2, 158.9, 154.7, 146.8, 138.9, 136.2, 132.0, 128.0, 122.8, 120.5, 117.7, 112.1, 105.2, 99.3, 56.0, 56.7; HRMS: $C_{17}H_{13}BrO_5$ *m*/*z* $[M + H]^+$: cal.:377.0024; found: 377.0017.

*2-(2-bromophenyl)-3-hydroxy-4H-chromen-4-one (**3f**).* Yellow solid; yield: 85%; FTIR (KBr) ν_{max}: 1598, 1456, 1305, 1207, 831, 771 cm^{-1}; ^1H NMR (400 MHz, $CDCl_3$/TMS): δ 8.26 (dd, $J = 1.2$ Hz, 8 Hz, 1H), 8.16 (d, $J = 8.8$ Hz, 2H), 7.7 (m, 1H), 7.68 (d, $J = 8.8$ Hz, 2H), 7.604 (d, $J = 8.4$ Hz, 1H), 7.45 (t, $J = 7.2$ Hz, 1H), 7.07 (s, 1H); ^{13}C NMR (100 MHz, $CDCl_3$/TMS): 155.4, 143.8, 138.5, 133.8, 131.9, 130.0, 129.2, 125.5, 124.7, 120.6, 118.2. HRMS: $C_{15}H_9BrO_3$ *m*/*z* $[M + H]^+$: calculated: 316.9814, found: 316.9809.

*2-(4-Bromophenyl)-3-hydroxy-6-methyl-4H-chromen-4-one (**3g**).* Yellow solid; yield: 87%; FTIR (KBr) ν_{max}: 3072, 2927, 1579, 1558, 1421, 1271, 835, 704 cm^{-1}; ^1H NMR (400 MHz, $CDCl_3$/TMS): δ 8.14 (d, $J = 8.4$ Hz, 2H), 8.01 (s, 1H), 7.66 (d, $J = 8.8$ Hz, 2H), 7.54 (m, 2H), 2.47 (s, 3H); ^{13}C NMR (100 MHz, $CDCl_3$/TMS): 173.3, 153.7, 143.6, 138.5, 135.3, 134.6, 131.8, 130.1, 129.1, 124.6, 124.5, 120.2, 118.0, 20.9; HRMS: $C_{16}H_{11}BrO_3$ *m*/*z* $[M + H]^+$: calculated: 330.9971, found: 330.9963.

General procedure for the synthesis of Suzuki coupled flavonols 5(a–n). Biaryl flavonols were synthesized by Suzuki–Miyaura cross-coupling with a slight modification in procedure based on the optimization reactions.[47] Flavonols **3(a–g)** 1 mm and substituted boronic acid **4(a–c)** were added to 4 mL 3 : 1 DMF : water mixture in a sealed tube. 1 mm of K_2CO_3 was added to it and stirred for a few minutes at room temperature. To this 10 mol percent of $Pd(OAc)_2$ was added and the reaction was kept for stirring at 100 °C for 5 h in a preheated oil bath. The reaction was monitored by thin-layer chromatography. After completion of the reaction, it was quenched with distilled water and separated by ethyl acetate. The crude product was purified by silica gel column chromatography to afford pure products **5(a–n)**. Eluent (hexane/ethyl acetate 12–15%). The products **5(a–n)** obtained were characterized by spectroscopic techniques.

*2-(2,4-Dimethoxyphenyl)-3-hydroxy-6-phenyl-4H-chromen-4-one (**5a**).* White solid; yield: 81%; FTIR (KBr) ν_{max}: 3300, 2924, 2852, 1712, 1606, 1463, 1386, 1294, 1193, 1029, 761, 611 cm^{-1}; ^1H NMR (400 MHz, $CDCl_3$/TMS): δ 8.47 (s, 1H), 7.92 (d, $J = 8.8$ Hz, 1H), 7.69 (d, $J = 8$ Hz, 2H), 7.59 (m, 2H), 7.50 (t, $J = 7.6$ Hz, 2H), 7.41 (d, $J = 6.4$ Hz, 1H), 6.66 (d, $J = 8.4$ Hz, 1H), 6.60 (s, 1H), 6.44 (s, 1H), 3.89 (s, 3H), 3.87 (s, 1H); ^{13}C NMR (100 MHz, $CDCl_3$/TMS): 162.9, 158.8, 155.3, 146.2, 139.4, 138.7, 137.4, 132.2, 131.9, 129.0, 127.8, 127.2, 123.1, 121.5, 118.9, 105.0, 99.2, 55.9, 55.5; HRMS: $C_{23}H_{18}O_5$ *m*/*z* $[M + H]^+$: calculated: 375.1232, found: 375.1254.

*3-Hydroxy-6-phenyl-2-(2,4,5-trimethoxyphenyl)-4H-chromen-4-one (**5b**).* White solid; yield: 80%; FTIR (KBr) ν_{max}: 3271, 2931, 2845, 1734, 1600, 1562, 1467, 1438, 1379, 1201, 1163, 1026, 827, 759, 694, 603 cm^{-1}; ^1H NMR (400 MHz, $CDCl_3$/TMS): δ 8.49 (d, $J = 2.4$ Hz, 1H), 7.94 (d, $J_{12} = 2.4$ Hz, $J_{14} = 8.8$ Hz, 1H), 7.70 (d, $J = 7.2$ Hz, 2H), 7.61 (d, $J = 8.8$ Hz, 1H), 7.50 (t, $J = 7.6$ Hz, 2H), 7.41 (t, $J = 7.6$ Hz, 1H), 7.14 (s, 1H), 6.67 (s, 1H), 6.51 (s, 1H), 3.97 (s, 3H), 3.90 (s, 3H), 3.89 (s, 3H); ^{13}C NMR (100 MHz, $CDCl_3$/TMS): 173.1, 152.5, 152.0, 143.2, 138.3, 137.5, 132.3, 129.0, 127.8,

127.2, 123.2, 118.9, 113.3, 110.9, 98.0, 57.1, 56.6, 56.1; HRMS: $C_{24}H_{20}O_6$ *m*/*z* $[M + H]^+$: calculated: 405.1338, found: 405.1365.

*3-Hydroxy-6-phenyl-2-(2,3,4-trimethoxyphenyl)-4H-chromen-4-one (**5c**).* White solid; yield: 81%; FTIR (KBr) ν_{max}: 3230, 2918, 2848, 1703, 1602, 1566, 1462, 1392, 1263, 1170, 1105, 840, 808, 763, 692 cm^{-1}; ^1H NMR (400 MHz, $CDCl_3$/TMS): δ 8.49 (d, J = 2.4 Hz, 1H), 7.94 (d, J = 2.4 Hz, 8.8 Hz, 1H), 7.70 (d, J = 8.9 Hz, 2H), 7.60 (d, J = 8.8 Hz, 1H), 7.50 (t, J = 7.2 Hz, 2H), 7.41 (t, J = 8 Hz, 2H), 6.84 (d, J = 8.8 Hz, 1H), 6.59 (s, 1H), 4.00 (s, 3H), 3.94 (s, 3H); ^{13}C NMR (100 MHz, $CDCl_3$/TMS): 173.4, 155.9, 155.4, 152.5, 146.0, 142.7, 139.4, 138.8, 137.7, 132.5, 129.1, 128.1, 128.1, 128.0, 127.3, 125.7, 123.3, 121.6, 119.0, 117.5, 107.5, 61.7, 61.0, 56.3; HRMS: $C_{24}H_{20}O_6$ *m*/*z* $[M + H]^+$: calculated: 405.1338, found: 405.1363.

*3-Hydroxy-6-phenyl-2-(2,4,6-trimethoxyphenyl)-4H-chromen-4-one (**5d**).* White solid; yield: 83%; FTIR (KBr) ν_{max}: 3273, 2918, 2848, 1724, 1631, 1604, 1581, 1467, 1294, 1224, 1201, 1109, 1035, 948, 806, 759, 690 cm^{-1}; ^1H NMR (400 MHz, $CDCl_3$/TMS): δ 8.493 (d, J = 2.4 Hz, 1H), 7.914 (d, J = 2.4 Hz, 8.8 Hz, 1H), 7.69 (d, J = 8.8 Hz, 2H), 7.59 (d, J = 8.8 Hz, 1H), 7.50 (t, J = 7.6 Hz, 2H), 7.41 (d, J = 7.2 Hz, 1H), 6.32 (s, 1H), 6.23 (s, 2H), 3.88 (s, 3H), 3.80 (s, 3H); ^{13}C NMR (100 MHz, $CDCl_3$/TMS): 173.4, 163.8, 159.8, 156.0, 144.0, 140.2, 139.1, 137.4, 132.1, 129.1, 127.8, 127.3, 123.3, 121.8, 119.3, 91.0, 56.2, 55.6; HRMS: $C_{24}H_{20}O_6$ *m*/*z* $[M + H]^+$: calculated:. 405.1338, found: 405.1361.

*2-(3,4-Dimethoxyphenyl)-3-hydroxy-6-phenyl-4H-chromen-4-one (**5e**).* White solid; yield: 84%; FTIR (KBr) ν_{max}: 3153, 2926, 2868, 1714, 1598, 1554, 1514, 1436, 1384, 1261, 1022, 765, 698 cm^{-1}; ^1H NMR (400 MHz, $CDCl_3$/TMS): δ 8.45 (d, J = 1.6 Hz, 1H), 7.95 (t, J = 8 Hz, 2H), 7.88 (s, 1H), 7.70 (m, 3H), 7.51 (t, J = 7.6 Hz, 2H), 7.42 (d, J = 8 Hz, 1H), 7.04 (d, J = 8.4 Hz, 2H), 4.01 (s, 3H), 3.98 (s, 3H); ^{13}C NMR (100 MHz, $CDCl_3$/TMS): 173.1, 154.6, 150.8, 148.8, 145.2, 139.2, 137.7, 132.4, 129.0, 127.9, 127.2, 123.1, 121.5, 120.8, 118.7, 110.9, 110.7, 56.0, 56.0; HRMS: $C_{23}H_{18}O_5$ *m*/*z* $[M + H]^+$: calculated: 375.1232, found: 375.1255.

*4-(3-Hydroxy-4-oxo-2-(2,4,5-trimethoxyphenyl)-4H-chromen-6-yl)benzonitrile (**5f**).* White solid; yield: 76%; FTIR (KBr) ν_{max}: 3305, 2922, 2852, 2223, 1722, 1602, 1568, 1514, 1460, 1415, 1261, 1209, 1159, 1020, 819, 786, 644 cm^{-1}; ^1H NMR (400 MHz, $CDCl_3$/TMS): δ 8.51 (d, J = 2.4 Hz, 1H), 7.92 (dd, J = 2 Hz, 8.8 Hz, 1H) 7.78 (s, 4H), 7.65 (d, J = 8.8 Hz, 1H), 7.14 (s, 1H), 6.67 (s, 1H), 6.49 (s, 1H), 3.98 (s, 3H), 3.90 (s, 6H); ^{13}C NMR (100 MHz, $CDCl_3$/TMS): 156.0, 152.7, 143.9, 143.4, 135.5, 132.9, 132.0, 127.9, 124.1, 119.6, 113.5, 111.6, 98.1, 57.2, 56.7, 56.3; HRMS: $C_{25}H_{19}NO_6$ *m*/*z* $[M + H]^+$: calculated: 430.129, found: 430.130.

*4-(3-Hydroxy-4-oxo-2-(2,3,4-trimethoxyphenyl)-4H-chromen-6-yl)benzonitrile (**5g**).* White solid; yield: 73%; FTIR (KBr) ν_{max}: 3633, 3302, 2924, 2862, 2225, 1705, 1595, 1566, 1290, 1209, 1097, 819, 785 cm^{-1}; ^1H NMR (400 MHz, $CDCl_3$/TMS): δ 7.98 (s, 1H), 7.40 (d, J = 8.8 Hz, 1H), 7.37 (s, 1H), 7.11 (s, 1H), 7.10 (s, 1H), 6.87 (d, J =, 2H), 6.73 (s, 1H), 6.48 (s, 1H), 6.32 (s, 1H), 3.47 (s, 3H), 3.42 (s, 3H), 3.40 (s, 3H); ^{13}C NMR (100 MHz, $CDCl_3$/TMS): 173.1, 155.9, 152.5, 143.9, 142.7, 138.9, 135.6, 132.9, 132.1, 129.6, 127.9, 125.7, 124.1, 121.8, 119.5, 117.3, 111.7, 107.5, 61.8, 61.0, 56.3; HRMS: $C_{25}H_{19}NO_6$ *m*/*z* $[M + H]^+$: calculated: 430.129, found: 430.1299.

*4-(3-Hydroxy-4-oxo-2-(2,4,6-trimethoxyphenyl)-4H-chromen-6-yl)benzonitrile (**5h**).* White solid; yield: 75%; FTIR (KBr) ν_{max}: 3288, 2945, 2225, 1600, 1568, 1483, 1408, 1292, 1095, 815, 642 cm^{-1}; ^1H NMR (400 MHz, $CDCl_3$/TMS): δ 8.50 (d, J = 2 Hz, 1H), 7.92 (dd, J = 2.4 Hz, J = 8.8 Hz, 1H), 7.78 (s, 4H), 7.64 (d, J = 8 Hz), 7.39 (d, J = 8.8 Hz, 1H), 6.84 (d, J = 8.8 Hz, 1 Hz), 6.59 (s, 1H), 4.00 (s, 3H), 3.95 (s, 3H), 3.93 (s, 3H); ^{13}C NMR (100 MHz, $CDCl_3$/TMS): 173.1, 155.9, 152.5, 143.9, 142.7, 138.9, 135.6, 132.9, 132.1, 129.6, 127.9, 125.7, 124.1, 121.8, 119.5, 117.3, 111.7, 107.5, 61.8, 61.0, 56.3; HRMS: $C_{25}H_{19}NO_6$ *m*/*z* $[M + H]^+$: calculated: 430.1291, found: 430.1296.

*Characterization data of 4-(2-(3,4-dimethoxyphenyl)-3-hydroxy-4-oxo-4H-chromen-6-yl)benzonitrile (**5i**).* White solid; yield: 74%; FTIR (KBr) ν_{max}: 3265, 3005, 2839, 1600, 1558, 1516, 1483, 1408, 1350, 1282, 1261, 1209, 1176, 1020, 858, 756, 705, 630 cm^{-1}; ^1H NMR (400 MHz, $CDCl_3$/TMS): δ 8.46 (s, 1H), 7.92 (m, 2H), 7.87 (s, 1H), 7.78 (s, 4H), 7.72 (d, J = 8.8 Hz, 1H), 7.05 (d, J = 8.4 Hz, 2H), 4.00 (s, 3H), 3.98 (s, 3H); ^{13}C NMR (100 MHz, $CDCl_3$/TMS): 172.9, 155.2, 151.0, 148.9, 145.5, 143.7, 137.9, 135.5, 132.1, 127.7, 123.8, 123.4, 121.6, 121.0, 119.2, 118.7, 111.6, 110.9, 110.7, 56.08, 56.03; HRMS: $C_{24}H_{17}NO_5$ *m*/*z* $[M + H]^+$: calculated: 400.1185, found: 400.1200.

*3-Hydroxy-6-(4-methoxyphenyl)-2-(2,4,6-trimethoxyphenyl)-4H-chromen-4-one (**5j**).* White solid; yield: 85%; FTIR (KBr) ν_{max}: 2922, 2852, 1712, 1602, 1460, 1377, 1247, 1159, 908, 734 cm^{-1}; ^1H NMR (400 MHz, $CDCl_3$/TMS): δ 8.43 (d, J = 2 Hz, 1H), 7.87 (dd, J = 2.4 Hz, 8.8 Hz, 1H), 7.63 (d, J = 8.4 Hz, 2H), 7.56 (d, J = 8.8 Hz, 1H), 7.02 (d, J = 8.4 Hz, 3H), 6.23 (s, 2H), 3.87 (s, 3H), 3.87 (s, 3H), 3.79 (s, 3H); ^{13}C NMR (100 MHz, $CDCl_3$/TMS): 173.4, 163.8, 159.8, 155.7, 144.0, 140.2, 136.1, 131.8, 128.4, 124.9, 122.5, 121.8, 119.2, 114.5, 91.0, 56.2, 55.6, 55.5; HRMS: $C_{25}H_{22}O_7$ *m*/*z* $[M + H]^+$: calculated: 435.1645, found: 435.1461.

*2-(3,4-Dimethoxyphenyl)-3-hydroxy-6-(4-methoxyphenyl)-4H-chromen-4-one (**5k**).* White solid; yield: 82%; FTIR (KBr) ν_{max}: 3277, 3219, 3176, 2954, 2922, 2852, 1726, 1597, 1560, 1512, 1462, 1379, 1246, 1174, 804, 765, 611 cm^{-1}; ^1H NMR (400 MHz, $CDCl_3$/TMS): δ 8.39 (d, J = 2 Hz, 1H), 7.92 (m, 2H), 7.87 (s, 1H), 7.65 (m, 3H), 7.025 (t, J = 7.2 Hz, 3H), 4.00 (s, 3H), 3.98 (s, 3H), 3.87 (s, 3H); ^{13}C NMR (100 MHz, $CDCl_3$/TMS): 173.3, 159.7, 154.4, 150.9, 149.4, 145.4, 137.9, 137.4, 132.3, 131.8, 128.3, 123.8, 122.4, 121.6, 120.9, 118.7, 114.60, 111.0, 110.8, 56.19, 56.13, 55.5; HRMS: $C_{24}H_{20}O_6$ *m*/*z* $[M + H]^+$: calculated: 405.1338, found: 405.1385.

*3-Hydroxy-6-(4-methoxyphenyl)-2-(2,3,4-trimethoxyphenyl)-4H-chromen-4-one (**5l**).* White solid; yield: 83%; FTIR (KBr) ν_{max}: 3307, 2943, 2841, 1602, 1566, 1463, 1409, 1298, 1180, 941, 823, 640 cm^{-1}; ^1H NMR (400 MHz, $CDCl_3$/TMS): δ 8.432 (d, J = 2 Hz, 1H), 7.87 (d, J = 2 Hz, J = 8.8 Hz, 1H), 7.63 (d, J = 8.8 Hz, 2H), 7.56 (d, J = 8.8 Hz, 1H), 7.02 (d, J = 8.4 Hz, 3H), 6.23 (s, 2H), 3.88 (s, 3H), 3.87 (s, 3H), 3.79 (s, 3H); ^{13}C NMR (100 MHz, $CDCl_3$/TMS): 173.4, 163.8, 159.8, 155.7, 144.0, 140.2, 136.1, 131.8, 128.4, 124.9, 122.5, 121.8, 119.2, 114.5, 91.0, 56.2, 55.6, 55.5; HRMS: $C_{25}H_{22}O_7$ *m*/*z* $[M + H]^+$: calculated: 435.1445, found: 435.1449.

*Characterization data of 2-([1,1′-biphenyl]-4-yl)-3-hydroxy-6-methyl-4H-chromen-4-one (**5m**).* White solid; yield: 79%; FTIR

(KBr) ν_{max}: 3234, 2918, 2848, 1703, 1604, 1566, 1487, 1454, 1392, 1261, 1170, 1105, 840, 810, 763, 688 cm^{-1}; ^1H NMR (400 MHz, $CDCl_3$/TMS): δ 8.35 (d, J = 8 Hz, 2H), 8.038 (s, 1H), 7.77 (d, J = 8 Hz, 1H), 7.68 (d, J = 8 Hz, 2H), 7.52 (m, 4H), 7.41 (d, J = 12 Hz, 1H), 7.16 (s, 1H), 2.49 (s, 3H); ^{13}C NMR (100 MHz, $CDCl_3$/TMS): 173.3, 153.8, 144.7, 142.7, 140.1, 138.5, 135.1, 134.5, 130.0, 128.9, 128.1, 127.9, 127.2, 127.1, 124.5, 120.4, 118.0, 20.9; HRMS: $C_{22}H_{16}O_3$ m/z $[M + H]^+$: calculated: 329.1177, found: 329.1206.

2-([1,1′-Biphenyl]-2-yl)-3-hydroxy-4H-chromen-4-one ***(5n)***. White solid; yield: 72%; FTIR (KBr) ν_{max}: 3078, 2922, 2852, 1708, 1597, 1552, 1473, 1436, 1249, 1193, 1114, 8.6, 758, 696 cm^{-1}; ^1H NMR (400 MHz, $CDCl_3$/TMS): δ 8.37 (d, J = 12 Hz, 2H), 8.28 (d, J = 8 Hz, 1H), 7.79 (d, J = 8 Hz, 2H), 7.75 (t, J = 8 Hz, 1H), 7.69 (d, J = 8 Hz, 2H), 7.64 (d, J = 8 Hz, 1H), 7.51 (t, J = 8 Hz, 2H), 7.45 (m, 2H), 7.09 (s, 1H); ^{13}C NMR (100 MHz, $CDCl_3$/TMS): 163.9, 155.7, 134.0, 133.8, 131.2, 130.5, 130.0, 128.6, 128.3, 126.2, 125.2, 123.7, 118.5; HRMS: $C_{21}H_{14}O_3$ m/z $[M + H]^+$: calculated: 315.1021, found: 315.1031.

Preparation of test compounds

Fourteen novel compounds were tested **5(a–n)**. The compounds were synthesized at the Department of Chemistry, School of Advanced Sciences, Vellore Institute of Technology (VIT), Vellore, India.

Determination of minimum inhibitory concentrations (MIC)

The broth dilution method described by the Clinical and Laboratory Standards Institute (CLSI) was used to determine the minimum inhibitory concentration (MIC).[48] The MIC of the compounds was determined to be the lowest concentration of the Suzuki-linked compounds **5(a–n)** which prevented the test bacterium *Pseudomonas aeruginosa* PAO1 from growing visibly. In a nutshell, 1 mg mL^{-1} of the compounds **5(a–n)** were dissolved in DMSO. Serial dilutions were performed in sterile Luria–Bertani broth in 96 well plate for the determination of MIC value. Gentamicin was used as the positive control of the experiment due to its reported antibiofilm activity and additionally due to its efficiency towards Gram-negative bacterial inhibition. 100 μL of bacterial culture was added to 100 μL of serially diluted compounds in 96 well plates. Later the plates were incubated for 24 h at 35 °C. Each test was done in triplicates.

Evaluation of the growth curve

A growth assay was performed to find the effect of $\frac{1}{2}$ MIC, 1/4 MIC, and 1/8 MIC dosages of test compounds on the growth of *P. aeruginosa*. Overnight grown test organism was treated with different concentrations including $\frac{1}{2}$ MIC, $\frac{1}{4}$ MIC, and 1/8 MIC doses of compounds **5(a–n)**. All the cultures including the untreated control were incubated at 37 °C and OD was noted each 2 h starting from 0 h at 600 nm.[49]

Biofilm prevention assay

Biofilm prevention assay was done by previously reported protocol.[50] *P. aeruginosa* bacterial strain was cultured in LB medium at 37 °C for 24 hours. A 1 : 100 dilution of these bacterial suspensions in LB broth with a turbidity of 0.1 OD was used for the assay. To evaluate the antibiofilm activity of the compounds, diluted bacterial suspension and MIC dose of test compounds were added to the flat bottom 96 well plate. To enable biofilm formation, the plates were incubated for 24 hours at 37 °C. The contents of each well were taken out after incubation, and the wells were then washed twice with a sterile LB medium. The plate was then air-dried and stained for 30 minutes at room temperature with 0.1 percent w/v crystal violet (CV) solution. The excess stain of CV was then rinsed with distilled water. 125 μL of 30% acetic acid was added to this well to solubilize the CV dye stained on the biofilm biomass and left for 15 minutes. A microplate reader was then used to measure the absorbance at 570 nm. Comparisons of the optical densities of drug-treated and untreated bacterial cultures were conducted and the percentage inhibition of biofilm biomass was determined by the following equation.

$$\%\ \text{Biofilm inhibition} = \frac{\text{OD untreated} - \text{OD treated}}{\text{OD untreated}} \times 100$$

Eradication activity of the compounds against preformed biofilms

Compounds **5(a–n)** were studied for their effect on eradicating preformed biofilms at their $\frac{1}{4}$ MIC doses by previously reported protocol.[51] A bacterial suspension of 0.1 OD was obtained and 100 μL of test bacterial suspension was added to the wells of a 96-well plate, and incubated for 24 h to allow initial bacterial adhesion and biofilm formation. Further, the content of the wells was removed, washed with sterile LB broth twice, and then filled with fresh LB broth containing $\frac{1}{4}$ MIC doses of compounds **5(a–n)**. Further, the plates were sealed and incubated at 37 °C for another 24 h. After the incubation, 96 well plate was processed and the percentage biofilm biomass reduction was calculated as reported above.

Analysis of biofilm architecture

Scanning electron microscopy. The test was carried out according to the method described earlier with minor modifications.[52] The bacterial strain was incubated in LB broth at 37 °C for 24 h. The culture broth was then diluted to achieve an OD of 0.1 with sterile LB media. The diluted bacterial suspension (2 mL) was then added to 24 well plates over 18 × 18 mm coverslips loaded previously in the wells and allowed to grow for 72 h. After 72 h bacterial suspension was removed from the wells and washed twice with a sterile LB medium. The wells were then filled with sterile LB medium containing $\frac{1}{4}$ MIC dose of drugs. A control experiment was also performed without the addition of a drug to compare the effect of the compound on biofilm formation. After incubation of the 24 well plates for another 48 h, the coverslips were picked out with sterile forceps and placed in new 24 well plates. The planktonic cells were washed with a sterile medium and the biofilm formed on the coverslips was fixed with 2% glutaraldehyde and dehydrated with varying percentages of ethanol (30%, 50%, 70%, 90%, and 100%). To evaluate biofilm formation and to compare it with biofilm

untreated with drug the SEM images were taken at SEM facilities at Vellore Institute of Technology.

Confocal laser scanning microcopy. Bacterial strain was incubated for 24 h at 37 °C. The bacterial suspension was then diluted to achieve an OD of 0.1. The diluted bacterial suspension (8 mL) along with $\frac{1}{4}$ MIC dosage of test compound was then transferred to a 50 mL sterile centrifuging tube and a clean coverslip was inserted into it. A control without the addition of any compounds was also incubated along with this. After 72 h of incubation the planktonic cells were removed by sterile water and the biofilm was stained using 0.1% acridine orange. The coverslips were then placed over a glass plate and the biofilm was visualized using confocal laser scanning microscope (Olympus Confocal Laser Scanning Microscope – Fluoview FV3000) with an excitation filter (515–560 nm) at a magnification of 60×.[53]

Anti-virulence testing

Effect of compounds on pyocyanin production. The test was carried out according to the method described earlier with minor modifications.[54] In brief, pyocyanin was extracted using chloroform from 24 h grown bacterial isolate in LB broth, supplemented with and without tested compounds **5(a–n)**. After centrifugation at 3000 rpm for 10 min, the bluish chloroform phase was isolated and treated with 0.2 M HCl. The content was vortexed vigorously for 10 s until the extraction of a pinkish upper phase. About 100 μL of the pinkish upper layer of all the samples was then transferred to 96 well plates and the OD at 690 nm was measured using a microplate reader. Variation in pyocyanin production in treated bacteria was measured in comparison with untreated control. Every experiment was repeated three times.

Effect of compounds on LasA protease production. LasA protease activity was determined by measuring the staphylolytic activity of cell-free supernatants of the test organisms that were treated and untreated with compounds **5(a–n)**. Cell-free culture supernatants (100 μL) were added to 900 μL of boiled *Staphylococcus aureus* cells. The optical density at 600 nm was measured after 60 min incubation and the protease activity was measured in comparison with the test compounds untreated control.[54]

Effect of compounds on cell surface hydrophobicity. Compounds **5(a–n)** were used to study cell hydrophobicity using bacterial cultures that were initially treated or untreated with sub-MIC doses of compounds. The compounds **5(a–n)** 100 μL at $\frac{1}{4}$ MIC was mixed vigorously with toluene (100 μL) for 2 min. Absorbance of the aqueous phase was recorded at OD_{600} to determine the cell surface hydrophobicity. Each experiment was repeated thrice for triplicates.[55]

Effect of compounds on rhamnolipid production. Rhamnolipid was estimated by the reported orcinol method in the cell-free supernatant of *P. aeruginosa*.[56] 1 mL bacterial supernatant treated and untreated with compounds **5(a–n)** incubated overnight. The overnight grown culture was then extracted twice using 1 mL of ethyl acetate. The organic layer was then separated and evaporated to dryness. The residue obtained from this organic phase was then dissolved in 500 μL of distilled water. 100 μL of this sample was then treated with 900 μL of 0.19% orcinol in 53% v/v H_2SO_4. The mixture was then heated for 30 minutes in the water bath at 80 °C, cooled and the absorbance was noted at 420 nm for the estimation of rhamnolipid.

Effect of compounds on gene expression level of *P. aeruginosa* PAO1 – real time polymerase chain reaction. *P. aeruginosa* PAO1 was incubated overnight and then treated in the culture with MIC dosage of compounds **5f** and **5m**. The culture was again incubated for 15 h and then centrifuged and the pellet was used for the following RNA isolation step. RNA was isolated by TRIzol method and the purity and quantity of RNA were identified by nanodrop, Biospectrometer, and Eppendorf. The 1000 ng of RNA isolated was converted to cDNA on the same day with Prime Script RT reagent Kit (Perfect Real Time) kit, Takara, with the manufacturer's instruction. Gene expression studies for the *rhlA* and *lasB* genes were performed on RT-PCR, Biorad, India, where, the *rpoD* gene was used as the control gene.[57] The primers used and the primer sequence is listed in Table 6.

Cytotoxicity of the compounds – MTT assay. Cytotoxicity of the compound **5f** was evaluated through MTT assay in HEK 293 cell lines. The cells (5×10^3 cells per well in 200 μL of media) were seeded onto 96 well plates and were allowed to grow for 24 h at 37 °C, 5% CO_2. Cells were treated with the increasing concentration of compound **5f** for 24 h and 48 h. The study was conducted in triplicates. DMSO, media were used as negative control, and cisplatin was used as a standard drug respectively. After 24 h and 48 h, 20 μL of MTT reagent (5 mg mL^{-1} in sterile distilled water) was added to each well and plates were wrapped with aluminium foil and was incubated for 4 h at 37 °C. The purple formazan product was dissolved by the addition of 100 μL DMSO to each well. The absorbance was measured using a micro plate reader (TECAN INFINITE M Plex, Switzerland) at 595 nm. Data were collected for three replicates each and used to calculate the mean. The percentage of live cells was calculated from this data, using the formula.[58]

$$\text{Percentage of live cells} = \frac{\text{mean OD of treated cells}}{\text{mean OD of untreated cell}} \times 100$$

IC_{50} values were calculated using dose response inhibition curves in Graphpad prism.

Molecular docking. Molecular docking studies were accomplished with the glide module from Schrodinger. The 3D structures of receptors involved in quorum-sensing were taken from Protein Data Bank (PDB IDs LasR: 2UV0, PqsR: 4JVI, RhlR: 8DQ0). The structures were prepared at physiological pH of 7.4

Table 6 List of primer sequences for *lasB*, *rhlA*, and pqsE genes used for gene expression study. *rpoD* gene was used as a control gene

	Primers	
	Forward	Reverse
rpoD	TCCACCGACAACAG	GAGCTGGAAACCGTGGACT
lasB	CGCAAGACCGAGAATGACA	AGACCAGTTGGGCGATGTT
rhlA	AAGCCAGCAACCATCAGC	GCACCTGGTCGATGTGAAA
pqsE	ATGATGACCTGTGCCTGTTG	CAGTGGTCGTAGTGCTTGTG

to add the missing residues, hydrogens and charges. The structures thus processed were then optimized by the OPLS4 force field to minimize the strain. Likewise, the ligand structures **5m** and **5f** were created in order to transform them into three-dimensional form and then produce potential conformations and protonation states within the physiological pH range. The binding site for our molecule was created by taking use of the co-crystal site. The extra precision protocol was used for the docking, and the molecules with higher docking scores were selected.

Molecular dynamics. An extensive 200 ns molecular dynamics of 2UV0-**5m**, 4JVI-**5m**, and 8DQ0-**5m** complexes was performed using the Desmond program from Schrodinge.[59] After the complex was solvated in SPC solvent, ions were added to the system in an orthorhombic periodic condition to neutralize it. Prior to the dynamics, the system was minimized using a quick 100 ps simulation. After that, the minimized complexes underwent through a production simulation using an NPT ensemble. This involved employing the Nose–Hoover chain thermostat and Martyna–Tobias–Klein barostat to keep the system's temperature at 300 K and its pressure at 1.01325 bars.

Binding free energy calculation. Molecular Mechanics Generalised Born and Surface Area (MM-GBSA) method was used to evaluate the binding free energy of the complex. The MD trajectory was extracted in 20 ns interval and MM-GBSA was calculated by providing VSGB solvent and 5 Å flexibility surrounding the ligand.[60]

The MM-GBSA is calculated as

$$\Delta G_{\text{bind}} = G_{\text{complex}} - G_{\text{protein}} - G_{\text{ligand}}$$

ΔG_{bind} – binding free energy, G_{complex}, G_{protein}, and G_{ligand} – free energies of complex, protein, and ligand, respectively.

Data analysis. All the experiments were done independently and the data obtained were expressed as mean ± standard deviation (SD) with a significant (p) value of 0.001 which is significant, using sigma plot 13.0, Systat Software, Inc. sigma plot for windows. All the results obtained in biofilm inhibition assay, static biofilm inhibition of preformed biofilm assay, and virulence factor estimation assays were analyzed using one-way ANOVA with Dunnett's method. Dunnett's method uses multiple comparisons *versus* control groups. Comparisons were performed within the biofilm production in different flavonols and that of the untreated control "(***$p < 0.001$)".

Conclusion

A set of biaryl flavonols were synthesized from substituted flavonols using a Suzuki–Miyaura cross-coupling reaction. The reaction gives excellent yields of the product in a ligand-free reaction methodology in DMF/aqueous solvent system using palladium acetate as the catalyst. All the products synthesized using this reaction methodology were utilized for the screening of antibiofilm and antivirulence activity against the opportunistic pathogen *Pseudomonas aeruginosa*. Compounds exhibited good antibiofilm and antivirulence activity against the test strain of bacteria. Virulence factors including pyocyanin, LasA protease, cell surface hydrophobicity and rhamnolipid were evaluated after treatment of the compounds. A molecular docking study was conducted to find the best ligands for LasR, RhlR, and PqsR. The molecular docking study revealed that contradictory to the *in vitro* studies, **5f** did not shows any pose towards the receptor proteins 2UV0 and 4JVI. But, the compound **5m** which was showing 80% biofilm inhibition was showing good binding affinity towards the receptor proteins and the compound was having high binding free energy in molecular dynamics study. Taking into consideration of the good binding affinity and high binding free energy, the compound **5m** was selected for the gene expression study and based on the highest antibiofilm activity of compound **5f** in *in vitro* study compound **5f** was also selected for gene expression study. The RT-PCR study of compounds **5f** and **5m** against *rhlA*, *lasB*, and *pqsE* shows downregulation in gene expression compared to the control. The gene expression study suggests that the anti-biofilm and antivirulence activity of the compounds are possibly due to the downregulation of genes and thereby inhibiting quorum sensing and biofilm formation. The cytotoxicity of the best compound **5f** was evaluated by MTT assay and found that the compound is nontoxic to living cells at their $\frac{1}{4}$ MIC dosage.

Conflicts of interest

The results of this paper are not affected by any competing financial interests or personal relationships.

Acknowledgements

The authors acknowledge the VIT management for providing lab and instrumental facilities, SIF and HOME for characterization techniques and VIT-SEED GRANT (No. SG20230044) for the financial support for completion of this project. ATB acknowledges VIT for awarding TRA fellowship.

References

1 C. C. C. J. Seechurn, M. O. Kitching, T. J. Colacot and V. Snieckus, *Angew. Chem., Int. Ed.*, 2012, **51**, 5062–5085.
2 F.-S. Han, *Chem. Soc. Rev.*, 2013, **42**, 5270–5298.
3 J. Magano and J. R. Dunetz, *Chem. Rev.*, 2011, **111**, 2177–2250.
4 N. Miyaura and A. Suzuki, *J. Chem. Soc. Chem. Commun.*, 1979, 866–867.
5 N. Miyaura and A. Suzuki, *Chem. Rev.*, 2002, **95**, 2457–2483.
6 A. Suzuki, *J. Organomet. Chem.*, 1999, **576**, 147–168.
7 A. J. J. Lennox and G. C. Lloyd-Jones, *Chem. Soc. Rev.*, 2013, **43**, 412–443.
8 J. P. G. Rygus and C. M. Crudden, *J. Am. Chem. Soc.*, 2017, **139**, 18124–18137.
9 C. Torborg and M. Beller, *Adv. Synth. Catal.*, 2009, **351**, 3027–3043.
10 V. Chandrasekhar, R. S. Narayanan and P. Thilagar, *Organometallics*, 2009, **28**, 5883–5888.

11 B. Bhayana, B. P. Fors and S. L. Buchwald, *Org. Lett.*, 2009, **11**, 3954–3957.
12 C. A. James, A. L. Coelho, M. Gevaert, P. Forgione and V. Snieckus, *J. Org. Chem.*, 2009, **74**, 4094–4103.
13 Y. J. Moon, X. Wang and M. E. Morris, *Toxicol. Vitro*, 2006, **20**, 187–210.
14 M. T. L. Ielpo, A. Basile, R. Miranda, V. Moscatiello, C. Nappo, S. Sorbo, E. Laghi, M. M. Ricciardi, L. Ricciardi and M. L. Vuotto, *Fitoterapia*, 2000, **71**, S101–S109.
15 C. X. Qin, X. Chen, R. A. Hughes, S. J. Williams and O. L. Woodman, *J. Med. Chem.*, 2008, **51**, 1874–1884.
16 L. Wang, T. Yi-Chen, T. Lian, H. Jing-Ting, Y. Jui-Hung and W. Ming-Jiuan, *J. Agric. Food Chem.*, 2006, **54**, 9798–9804.
17 S. Chirumbolo, *Inflammation Allergy: Drug Targets*, 2010, **9**, 263–285.
18 H. Matsuda, K. Ninomiya, H. Shimoda and M. Yoshikawa, *Bioorg. Med. Chem.*, 2002, **10**, 707–712.
19 L. Silver and K. Bostian, *Eur. J. Clin. Microbiol. Infect. Dis.*, 1990, **97**(9), 455–461.
20 C. Mouffouk, S. Mouffouk, S. Mouffouk, L. Hambaba and H. Haba, *Eur. J. Pharmacol.*, 2021, **891**, 173759.
21 L. Gao, Z. Tang, T. Li and J. Wang, *Microb. Pathog.*, 2023, **182**, 106165.
22 K. I. Arita-Morioka, K. Yamanaka, Y. Mizunoe, Y. Tanaka, T. Ogura and S. Sugimoto, *Sci. Rep.*, 2018, **8**, 1–11.
23 L. Gao, Z. Tang, T. Li and J. Wang, *Pathog. Dis.*, 2021, **79**, 1–10.
24 L. N. Silva, G. C. A. Da Hora, T. A. Soares, M. S. Bojer, H. Ingmer, A. J. Macedo and D. S. Trentin, *Sci. Rep.*, 2017, **7**, 1–16.
25 P. Krzyżek, P. Migdał, E. Paluch, M. Karwańska, A. Wieliczko and G. Gościniak, *Int. J. Mol. Sci.*, 2021, **22**, 1–19.
26 X. Wu, G. L. Ma, H. W. Chen, Z. Y. Zhao, Z. P. Zhu, J. Xiong, G. X. Yang and J. F. Hu, *J. Ethnopharmacol.*, 2023, **306**, 116177.
27 D. Ming, D. Wang, F. Cao, H. Xiang, D. Mu, J. Cao, B. Li, L. Zhong, X. Dong, X. Zhong, L. Wang and T. Wang, *Front. Microbiol.*, 2017, **8**, 1–11.
28 L. Slobodníková, S. Fialová, K. Rendeková, J. Kováč and P. Mučaji, *Molecules*, 2016, **21**, 1–15.
29 P. A. M. Gómez, L. Y. T. C. Jon, D. J. M. Torres, R. E. B. Amaranto, I. E. C. Díaz and C. A. M. Medina, *F1000Research*, 2021, **10**, 1–23.
30 R. Frei, A. S. Breitbach and H. E. Blackwell, *Angew. Chem., Int. Ed.*, 2012, **51**, 5226–5229.
31 P. Di Martino, *AIMS Microbiol.*, 2018, **4**, 274–288.
32 H. C. Flemming and J. Wingender, *Nat. Rev. Microbiol.*, 2010, **89**(8), 623–633.
33 A. H. Broderick, A. S. Breitbach, R. Frei, H. E. Blackwell and D. M. Lynn, *Adv. Healthcare Mater.*, 2013, **2**, 993–1000.
34 L. Lu, W. Hu, Z. Tian, D. Yuan, G. Yi, Y. Zhou, Q. Cheng, J. Zhu and M. Li, *Chin. Med.*, 2019, **14**, 1–17.
35 S. P. Diggle and M. Whiteley, *Microbiology*, 2020, **166**, 30–33.
36 J. P. Clancy, L. Dupont, M. W. Konstan, J. Billings, S. Fustik, C. H. Goss, J. Lymp, P. Minic, A. L. Quittner, R. C. Rubenstein and K. R. Young, *Thorax*, 2013, **68**, 818–825.
37 F. F. Tuon, L. R. Dantas, P. H. Suss and V. S. T. Ribeiro, *Pathogens*, 2022, **11**, 300–319.
38 K. P. Rumbaugh, J. A. Griswold and A. N. Hamood, *Microbes Infect.*, 2000, **2**, 1721–1731.
39 M. Malešević, F. D. Lorenzo, B. Filipić, N. Stanisavljević, K. Novović, L. Senerovic, N. Polović, A. Molinaro, M. Kojić and B. Jovčić, *Sci. Rep.*, 2019, **9**, 1–13.
40 N. R. Kishore, D. Ashok, M. Sarasija and N. Y. S. Murthy, *Chem. Heterocycl. Compd.*, 2018, **53**, 1187–1191.
41 D. Ashok, S. Ravi, B. V. Lakshmi and A. Ganesh, *J. Serb. Chem. Soc.*, 2015, **80**, 1361–1366.
42 H. Hu, C. Ge, A. Zhang and L. Ding, *Mol*, 2009, **14**, 3153–3160.
43 G. W. Lau, D. J. Hassett, H. Ran and F. Kong, *Trends Mol. Med.*, 2004, **10**, 599–606.
44 S. Hall, C. McDermott, S. Anoopkumar-Dukie, A. J. McFarland, A. Forbes, A. V. Perkins, A. K. Davey, R. Chess-Williams, M. J. Kiefel, D. Arora and G. D. Grant, *Toxins*, 2016, **8**, 236–250.
45 S. Lindsay, A. Oates and K. Bourdillon, *Int. Wound J.*, 2017, **14**, 1237–1247.
46 T. B. Anjitha, P. Shanmugam and K. R. Ethiraj, *ChemistrySelect*, 2021, **6**, 12074–12081.
47 L. Giordano, V. V. Shvadchak, J. A. Fauerbach, E. A. Jares-Erijman and T. M. Jovin, *J. Phys. Chem. Lett.*, 2012, **3**, 1011–1016.
48 J. B. Patel, G. M. Eliopoulos, S. G. Jenkins, F. S. J. Lewis II, P. B. Limbago, D. P. Nicolau, F. R. Patel, M. Powell, F. S. S. Richter, D. M. J. Swenson, M. M. M. Traczewski, M. D. J. Turnidge, M. P. Weinstein, B. L. Zimmer, D. M. A. Bobenchik, D. S. Campeau, D. K. S. Cullen, R. F. M. G. H. Gold, F. M. R. Humphries, D. J. T. Kirn, J. S. Lewis II, F. B. Limbago, A. J. Mathers, D. T. Mazzulli, F. S. S. Richter, F. M. Satlin, M. N. A. Schuetz and M. D. P. Tamma, *Performance standards for antimicrobial susceptibility testing*, Clinical and Laboratory Standards Institute (CLSI), 2016, vol. 40, pp. 100–125.
49 G. Maisetta, A. M. Piras, V. Motta, S. Braccini, D. Mazzantini, F. Chiellini, Y. Zambito, S. Esin and G. Batoni, *Microorganisms*, 2021, **9**, 912–930.
50 P. Rathinam and P. Viswanathan, *Int. J. Pharm. Pharmaceut. Sci.*, 2014, **6**, 85–90.
51 L. Kumar, S. Chhibber and K. Harjai, *Fitoterapia*, 2013, **90**, 73–78.
52 J. Zhou, S. Bi, H. Chen, T. Chen, R. Yang, M. Li, Y. Fu and A. Q. Jia, *Front. Microbiol.*, 2017, **8**, 769.
53 J. Rajkumari, C. M. Magdalane, B. Siddhardha, J. Madhavan, G. Ramalingam, N. A. Al-Dhabi, M. V. Arasu, A. K. M. Ghilan, V. Duraipandiayan and K. Kaviyarasu, *J. Photochem. Photobiol., B*, 2019, **201**, 111667.
54 V. Huerta, K. Mihalik, S. H. Crixell and D. A. Vattem, *Int. J. Appl. Res. Nat. Prod.*, 2008, **1**, 9–15.
55 M. Chatterjee, S. D'Morris, V. Paul, S. Warrier, A. K. Vasudevan, M. Vanuopadath, S. S. Nair, B. Paul-Prasanth, C. G. Mohan and R. Biswas, *Appl. Microbiol. Biotechnol.*, 2017, **101**, 8223–8236.

56 J. Luo, B. Dong, K. Wang, S. Cai, T. Liu, X. Cheng, D. Lei, Y. Chen, Y. Li, J. Kong and Y. Chen, *PLoS One*, 2017, **12**, e0176883.
57 B. Pejin, A. Ciric, J. Markovic, J. Glamoclija, M. Nikolic, B. Stanimirovic and M. Sokovic, *Curr. Pharm. Biotechnol.*, 2015, **16**, 733–737.
58 R. Kartikeyan, D. Murugan, T. Ajaykamal, M. Varadhan, L. Rangasamy, M. Velusamy, M. Palaniandavar and V. Rajendiran, *Dalton Trans.*, 2023, **52**, 9148–9169.
59 S. Genheden and U. Ryde, *Expert Opin. Drug Discovery*, 2015, **10**, 449–461.
60 S. V. Pattar, S. A. Adhoni, C. M. Kamanavalli and S. S. Kumbar, *Beni-Suef Univ. J. Basic Appl. Sci.*, 2020, **9**, 1–10.